Research Square

Preprints are preliminary reports that have not undergone peer review.
They should not be considered conclusive, used to inform clinical practice,
or referenced by the media as validated information.

Formulation, Optimization and Evaluation of Bioenhancer Integrated Curcumin Nanogel System for Psoriasis

Kamal Saroha

kamal@kuk.ac.in

Kurukshetra University

Shiv Kumar

Kurukshetra University

Deepika Aggarwal

Kurukshetra University

Research Article

Keywords: Box-Behnken design, Curcumin, Nanogel, Optimization, Piperine, Psoriasis, Anti-oxidant

Posted Date: July 30th, 2026

DOI: https://doi.org/10.21203/rs.3.rs-10408687/v1

License: This work is licensed under a Creative Commons Attribution 4.0 International License.
Read Full License

Additional Declarations: No competing interests reported.

Formulation, Optimization and Evaluation of Bioenhancer Integrated Curcumin Nanogel System for Psoriasis

Kamal Saroha[1*], Shiv Kumar[1], Deepika Aggarwal[1]

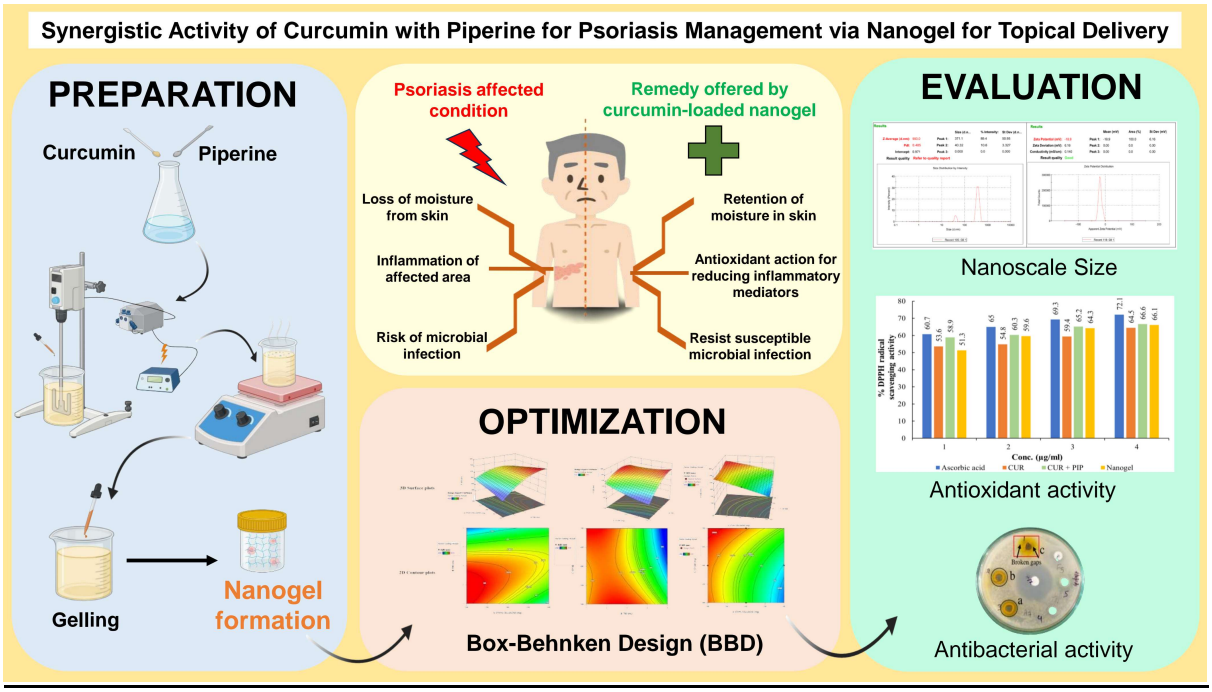
[1]**Institute of Pharmaceutical Sciences, Kurukshetra University, Kurukshetra-136119, Haryana, India**

Corresponding author: Kamal Saroha (kamal@kuk.ac.in)

ORCID: Kamal Saroha: https://orcid.org/0009-0004-9621-6902

Acknowledgement

Author Contributions: Kamal Saroha: Conceptualization and administration of this project. **Shiv Kumar:** Participated in writing, and editing manuscript. **Deepika Aggarwal:** Reviewing of the project.



Abstract

Background

Psoriasis is a relatively frequent chronic, immune-mediated inflammatory skin disease that displays epidermal hyperproliferation, rash, and moderate skin infection due to microbes. Despite its potent anti-inflammatory and antioxidant properties, curcumin suffers from poor aqueous solubility, rapid metabolism, and extensive first-pass effect, resulting in an oral bioavailability of less than 1%; piperine, a well-known bioenhancer derived from *Piper nigrum*, has been shown to significantly enhance curcumin bioavailability by inhibiting its metabolic degradation and improving intestinal absorption. Both of these possesses relevant activity to elevate symptoms related to psoriasis.

Objective

As a result of its association with cutaneous inflammation due to free radical generated, dehydration, and microbial susceptibility, the research work involves the development and assessment of curcumin-loaded nanogel with the aim of improving performance and topical drug release. Although psoriasis is not primarily a bacterial disease, disruption of the skin barrier in psoriatic lesions may increase susceptibility to secondary microbial colonization, particularly by *Staphylococcus aureus*. Therefore, the antibacterial activity of the developed nanogel was qualitatively evaluated as a supportive characteristic that may contribute to improved skin health and reduced microbial burden in psoriatic skin.

Method and Results

The study employs the emulsion-solvent diffusion method for formulating nanogels and optimizes it through a Box-Behnken design. The optimized nanogel was then assessed for particle size, zeta potential, viscosity, and drug content. We also performed Fourier-transform infrared spectroscopy, differential scanning calorimetry, and X-ray diffraction analysis. In addition, *in vitro* antimicrobial and antioxidant activities were assessed, along with a comparative evaluation of its *in vitro* drug release profile with a conventional curcumin gel.

The synthesized and selected optimized curcumin-loaded nanogel showed a nanoscale size of 593 nm, satisfactory stable zeta potential of -18.9 mV, and drug content of 70.3%. It displayed 24 h sustained release (65.56%) and occlusivity (56.09% measured within 6 h). Strong antioxidant activity of optimized nanogel, nearly equal to ascorbic acid, and superior antibacterial action, due to presence of piperine along with curcumin within nanogel, confirmed effective treatment approach showing a potential topical psoriasis treatment.

Conclusion

The bioenhancer-integrated curcumin nanogel exhibited sustained *in vitro* drug release, indicating its potential as a patient-friendly topical formulation approach for the effective delivery of curcumin.

Keywords: Box-Behnken design; Curcumin; Nanogel; Optimization; Piperine; Psoriasis; Anti-oxidant

1. Introduction

Psoriasis is characterized as a chronic inflammatory skin disorder that is marked by recurrent erythematous plaques with scaling and dryness. The disease is caused by immune dysregulation, resulting in the production of excessive pro-inflammatory cytokines, which result in abnormal proliferation of keratinocytes along with their impaired differentiation, resulting in disruption of the skin barrier [1]. These pathological changes lead to inflammation, dehydration, itching, and predisposing to microbial infections [2]. Despite the widespread use of

conventional topical formulations such as creams, ointments, and gels, these formulations suffer from limitations, such as insufficient penetration into the skin, poor drug retention inside psoriatic lesions, instability of active compounds, and the need for frequent application often yields suboptimal therapeutic outcomes. These challenges have encouraged the development of advanced delivery strategies that have the potential to enhance localization, stability, and extended release of the drug at its site of action [3]. Nanotechnology-based therapies and drug administration methods have emerged as an effective solution to address the constraints of the conventional topical formulations. By decreasing particle size to the nanometer (typically < 1000 nm) range, these systems improve drug solubility, protect unstable compounds, and increase penetration through the stratum corneum [4]. Among these systems, nanogels have gained attention due to their ability to combine nanoscale drug delivery with a hydrated gel matrix, offering controlled drug release, improved skin adhesion, enhanced hydration, and better patient acceptability, thereby improving therapeutic performance in topical applications. Nanogels are defined as three-dimensional networks of polymers that are less than one micron in size [5–7]. Nanogel encompassed of hydrogel particulate entities with a nanometer-sized space; therefore, possessing qualities of hydrogel and nanoparticle described above at the same time. Nanogels have the property of absorbing enormous volumes of water or biological fluids while preserving their structure, which is attributable to the presence of hydrophilic groups such as -OH, -CONH-, -$CONH_2$, and -SO_3H in the polymer [8]**.**

Phytochemicals have gained increasing attention in dermatological applications due to their multi-targeting therapeutic potential. However, they exhibit poor aqueous solubility, low permeability, and limited bioavailability, restricting their clinical effectiveness [9]. Curcumin, a polyphenolic compound derived from *Curcuma longa*, classified as a BCS class IV compound, indicating low solubility and low permeability, which significantly limits its topical bioavailability, is one such phytochemical with well-documented anti-inflammatory, antioxidant, immunomodulatory, and antimicrobial activities[10,11]. It modulates key molecular pathways involved in inflammatory skin disorders, such as inhibition of NF-κB and down-regulation of pro-inflammatory cytokines [12]. Further, the use of bioenhancers is an efficient approach to enhance the therapeutic performance of curcumin [13]. Piperine, a natural alkaloid found in *Piper nigrum*, enhances curcumin bioavailability by increasing membrane permeability and reducing metabolic degradation. When combined together, curcumin and piperine have been shown to have enhanced oral pharmacological efficacy, and therefore this combination is especially attractive for the management of inflammatory skin conditions [13,14]. However, topical delivery of such combinations is difficult with traditional dosage forms. Psoriasis comes with a change in skin physiology and this often makes conventional topical formulations ineffective. The use of nanogels offers controlled drug release, increased skin adhesion capacity, hydration, and patient acceptability. Their non-greasy nature, favorable rheological properties and especially their ability to have prolonged contact with the skin makes them particularly suitable for topical management of chronic inflammatory skin disorders over extended periods of time [15]. Despite the potential benefits of nanotechnology-based systems, there is a need for optimization of formulations capable of effective delivery of phytochemicals and addressing the limitations of conventional topical therapy. Therefore, the current work is dedicated to the development and evaluation of a curcumin-based nanogel with piperine incorporation, aiming at the improvement in drug delivery, making it a patient friendly and rational approach to manage psoriasis.

2. Materials and methods

2.1 Materials

We obtained curcumin and piperine from Sunpure Extracts Pvt. Ltd as a generous gift sample. Ethanol, Carbopol 940, and Tween 80 were purchased from Molychem. Ethyl cellulose, polyvinyl alcohol, triethanolamine, and methyl paraben were sourced from HiMedia. All the chemicals used during the study were of analytical grade.

2.2 Preformulation studies

2.2.1 Organoleptic evaluation

Organoleptic evaluation provides quick qualitative information about the drug based on sensory attributes–color, odor, and appearance. These characteristics are useful in identifying the quality of materials and detecting any physical changes that take place during storage or formulation [16].

2.2.2 UV-Visible spectroscopic analysis

UV-Visible spectroscopy was applied in order to characterize the absorption of curcumin and support the qualitative and quantitative analysis. UV-Visible spectrophotometer (Systronic, Model UV2206TS) was used to scan the sample from 200-900 nm. The absorption maximum (λ_{max}) was found by preparing and scanning a sample in methanol simultaneously against methanol (as blank). Identifying the value of λ_{max} guarantees that the spectrophotometric quantification can be accurately measured in subsequent studies [17].

2.2.3 Preparation of standard calibration curve

A calibration curve was constructed according to Beer-Lambert's law. A 100 µg/mL curcumin stock solution was prepared in methanol and diluted serially to prepare aliquots from 1-5 µg/mL. Absorbance was recorded at λ_{max} using methanol (as blank). A similar curve was drawn in a phosphate buffer (pH 6.5):ethanol mixture (7:3) using the same solvent ratio as blank. These curves were used as reference standards for quantitative analysis [17].

2.2.4 Solubility analysis

Solubility has an impact on the rate of dissolution, bioavailability, and formulation design. Curcumin's solubility was investigated in water, phosphate buffer (pH 6.5), methanol, ethanol, and phosphate buffer (pH 6.5):ethanol (7:3) mixture. Excess curcumin was added to 10 mL of each solvent, taken in 25 mL flasks, and shaken at room-temperature for 24 h. After being filtered through a 0.45 µm membrane filter, concentrations were measured by UV spectrophotometry. The data informs the choice of solvent and formulation design for dealing with curcumin's low water solubility [18].

2.2.5 Curcumin loaded-nanogel (CUR-NG) preparation

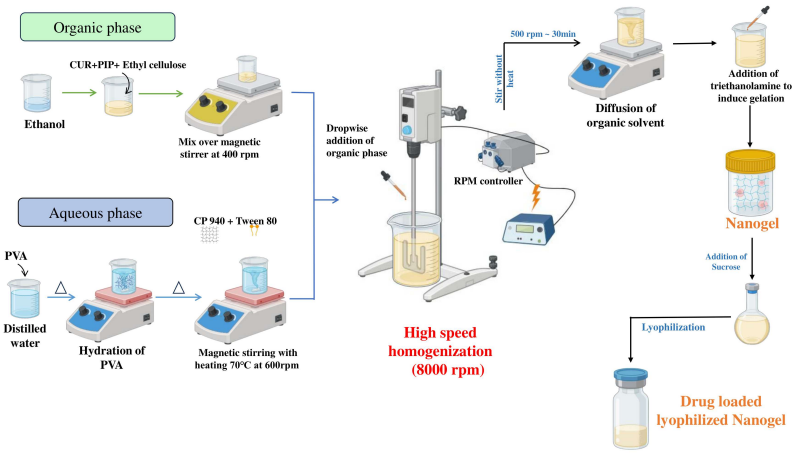


Fig. 1 Emulsion solvent diffusion method for nanogel preparation

Emulsion solvent diffusion method (Fig. 1) was employed to prepare CUR-NGs. This technique involves dispersing an organic phase, consisting of curcumin (100 mg), piperine (25 mg), and ethyl cellulose dissolved into 10 mL ethanol into an aqueous phase comprising of polyvinyl alcohol (PVA 0.5% w/w), Carbopol 940, and Tween 80 in a predefined required amount, with high-shear homogenization (~8000 rpm) facilitates nanoparticle formation. The values of ethyl cellulose, Tween 80, and Carbopol 940 were taken as mentioned in Table 1. Emulsification involved homogenizing the aqueous phase (20-25 °C) and adding the organic phase dropwise into the vortex. Post-homogenization, magnetic stirring (300-500 rpm, 30 min) promoted solvent diffusion. Gelation followed via dropwise triethanolamine addition (100-200 rpm) to reach pH 5-6. The resulting nanogel was stored in light-protected, airtight containers [19]. For further evaluation of surface morphology and crystalline state, selected (optimized) nanogel was lyophilized using sucrose (4% w/v) as cryoprotectant. Sucrose was dissolved in the nanogel, pre-frozen at -20 °C (24 h), and lyophilized (24 h) to produce free-flowing powder, stored refrigerated in airtight containers for characterization [20].

3. Optimization using Box-Behnken design (BBD)

Design-Expert Software version 13 (Stat-Ease Inc., Minneapolis, MN, USA) was utilized to optimize CUR loaded nanogels. To determine the effects of selected three independent variables on nanogel formulation, the Box-Behnken design (BBD) was used to optimize the process in terms of ethyl cellulose (Factor A) Tween 80 (Factor B) and Carbopol 940 (Factor C). All three factors were evaluated at three levels (−1, 0, and +1) during the optimization process, as demonstrated in Table 1. Other parameters of formulation and the processes remained constant in the study to encourage homogeneity. To examine how the three critical quality attributes were influenced by the chosen variables, 15 experimental runs were conducted in the focus of the optimization procedure [21]. The particle size, zeta potential, and viscosity were selected as the major parameters of the robustness and efficiency.

Table 1. Independent and dependent variables in experimental design for optimization

FORMULATION CODES	Design codes			Respective value		
	EC	**T 80**	**CP 940**	**EC (mg)**	**T 80 (mL)**	**CP 940 (mg)**
G1	-1	0	+1	100	3	700
G2	+1	+1	0	300	5	600
G3	0	0	0	200	3	600
G4	0	0	0	200	3	600
G5	+1	0	+1	300	3	700
G6	-1	0	-1	100	3	500
G7	+1	-1	0	300	1	600
G8	-1	-1	0	100	1	600
G9	0	+1	-1	200	5	500
G10	-1	+1	0	100	5	600
G11	+1	0	-1	300	3	500
G12	0	+1	+1	200	5	700
G13	0	-1	+1	200	1	700

G14	0	-1	-1	200	1	500
G15	0	0	0	200	3	600

Independent variables		**Design matrix codes**			**Dependent variables**
Description	**Units**	**Low (-1)**	**Centre (0)**	**High (+1)**	
Ethyl cellulose (EC)	mg	100	200	300	Particle size (Y1)
Tween 80 (T 80)	mL	1	3	5	Zeta potential (Y2)
Carbopol 940 (CP 940)	mg	500	600	700	Viscosity (Y3)

4. Selection and evaluation of formulated optimized nanogel

4.1 Organoleptic evaluation

Organoleptic evaluation of the prepared gel was done to check the physical properties of nanogel such as texture, color, and homogeneity. Texture and colour were visually evaluated to ensure the desired appearance and stability of the formulation. Homogeneity was determined by sampling about 1 g of gel from various parts of the container (middle, bottom, left, and right), spreading them on a glass slide and observing their uniformity and absence of particulate matter or phase separation [22].

4.2 Particle size, zeta potential and polydispersity index

A Malvern Zetasizer (Malvern, UK) was used to measure the particle size (measured in nm), zeta potential and polydispersive index (PDI) of the nanogels. Particle size and polydispersity index (PDI) were determined using dynamic light scattering (DLS) to assess size and distribution uniformity. To determine the surface charge and colloidal stability of the formulation, the zeta potential was measured. The samples were first diluted 100 times in distilled water to avoid multiple scattering effects before analysis. The samples that were diluted were put in disposable cuvettes and analyzed at the room temperature [23].

4.3 pH, spreadability, and viscosity

The pH of the nanogel formulations was determined using a calibrated digital pH meter (Perfit, India) for skin compatibility. The instrument was standardized using buffer solutions with pH 4.0, 7.0, and 9.2, and then used for pH analysis. A weighed quantity (5 g) of each nanogel was taken into a beaker, and the electrode was immersed directly into the sample to obtain the pH value [24].

The spreadability of the nanogel formulations was measured by the Slide-Slip method for ease of application. A fixed amount of nanogel was placed between two clean glass slides, and a weight of 20g was applied in order to spread it uniformly. The time required for the upper slide to slip off was recorded and a value for spreadability was calculated using the formula given below [25].

$$\boldsymbol{S} = M \times \frac{L}{T}$$

Where, S represents spreadability ($g \cdot cm \cdot sec^{-1}$), M = Weight tied to upper slide (g), L = Length of glass slides (cm), T = Time taken to separate the slides (sec)

The nanogel formulations were measured for their viscosity using a Brookfield Viscometer (DV-II+ PRO, Brookfield Engineering Laboratories, USA) using spindle 64. The formulations were equilibrated at 25 ± 1 ˚C for 30 min before measuring. The spindle was immersed centrally and rotated at 100 rpm until a constant reading was obtained. Viscosity assessment gives an insight into the rheological behavior of the nanogel that affects the spreadability, residence time on the skin, and overall topical performance [26].

The optimized formulation was chosen on the basis of dependent variables such as particle size, zeta potential and viscosity. The selected batch showed nanosized distribution with homogeneous distribution, suitable zeta potential that will give stability to the dispersion, and desired viscosity with shear-thinning behavior. These characteristics altogether met the essential requirements and meant that it was the most appropriate formulation for nanogels to be used in further studies.

4.4 Drug content of optimized nanogel

For the estimation of drug content, 100 mg of optimized CUR-NG was dispersed in 10 mL of methanol. The mixture was shaken uniformly for 30 minutes to ensure complete extraction and was filtered on a Whatman filter paper (0.45μm). The filtrate was suitably diluted twice, and scanned with UV spectroscopy at the determined λ_{max} and the absorbance values were recorded. The drug content was calculated using the standard curve equation [27].

4.5 Fourier transform infrared spectroscopy

Fourier transform infrared (FTIR) spectroscopy was performed in order to study potential interactions among curcumin, piperine, excipients, and the optimized CUR-NG formulation. FTIR spectra of pure curcumin, piperine, individual components of the formulation, were recorded and compared to existing data, to reveal the characteristic functional groups and any changes in peak position or intensity of the spectra. The analysis of optimized nanogel was also done by using an FTIR spectrometer (ABB MB3000, FT-IR Analyzer). Spectra were obtained over the wavenumber interval between 400-4000 cm^{-1} at a resolution of 4 cm^{-1} [28].

4.6 Powder X-ray diffraction

X-ray diffractometry (XRD) was used to study the crystalline nature of curcumin, piperine, and optimized CUR-NG. Powdered curcumin, piperine and the lyophilized nanogel were irradiated with x-ray rays and the diffraction patterns were recorded. This analysis gave good insight into the changes in crystallinity after formulation, which may have an impact on solubility, dissolution behavior, and overall bioavailability of the active compounds [29].

4.7 Differential scanning calorimetry

Differential scanning calorimetry (DSC) was conducted to analyze the thermal properties of curcumin, piperine and potential drug-polymer interaction in the nanogel formulation that had been developed. Pure curcumin, piperine and the optimized CUR-NG were analyzed by Discovery 25 (TA Instruments, USA). Each of the samples (approximately 5-7.5 mg) was weighed accurately and packed in aluminum pans. Scanning of samples was conducted at the temperature of 30-300 ℃/min and the heating rate of 10 ℃/min and the flow rate of nitrogen at 20 mL/min. The thermograms obtained were employed to determine the melting behavior, crystallinity as well as potential interactions between the drug and polymer [29].

4.8 Structure and morphology

The lyophilized optimized CUR-NG surface morphology was examined using a field emission scanning electron microscope (FE-SEM, JEOL 7610F Plus, Japan). The lyophilized samples were coated with a thin layer of gold by sputtering and attached to the aluminum stubs using the double-sided carbon adhesive tape for better surface conductivity. The magnification of the photomicrograph was chosen so as to assess the aspects of particle morphology, surface, and structure characteristics of nanogel formulation [30].

4.9 *In vitro* antibacterial evaluation

The antibacterial effect of optimized CUR-NG formulation was tested against *Staphylococcus aureus* (Gram-positive) which is prominently reported in literature to be associated with psoriasis lesions. Zones of inhibition were measured after incubation to measure the antibacterial activity of the formulation [31,32].

4.10 *In vitro* antioxidant assay

The antioxidant activity of the optimized CUR-NG was evaluated using the DPPH radical scavenging assay. A freshly prepared 0.1 mM DPPH solution (3.94 mg in 100 mL methanol) was protected from light. The stock solutions of optimized CUR-NG and ascorbic acid were prepared in methanol (0.1 mg/mL) and diluted to concentrations of 1, 2, 3, and 4 µg/mL. Equal volumes of DPPH solution and sample/standard were mixed and incubated in the dark at room temperature (25 ± 2 °C) for 30 min. Observations were recorded at 516 nm using a UV-visible spectrophotometer, with methanol as the blank, and radical scavenging activity was calculated [33,34].

$$\boldsymbol{DPPH\ inhibition}\ (\%) = 100 \times \frac{A_a - A_b}{A_a}$$

Where, A_a=Absorbance of the DPPH solution, A_b=Absorbance of sample

4.11 *In vitro* skin occlusivity method

The occlusive properties of the CUR-NG were evaluated using an *in vitro* occlusivity test. Briefly, 100 mL beakers were filled to half their volume with distilled water and covered with Whatman filter paper No. 41. A fixed quantity of CUR-NG (250 mg) was uniformly spread over the surface of the filter paper using a spatula, while control beakers were left without the formulation. All beakers were maintained at 37 ± 0.5 °C to simulate skin surface temperature. The beakers were weighed at predetermined intervals (0, 6, and 24 h), and the extent of water loss due to evaporation was calculated to assess the occlusive effect of the nanogel [27,35].

$$\boldsymbol{F} = \frac{(A - B)}{A} \times 100$$

Where, A = Water loss with the test sample (g) and B = Water loss with control (g)

4.12 *In vitro* drug release and kinetics assessment

In vitro drug release of curcumin was evaluated using a Franz diffusion cell with a receptor compartment volume of 30 mL and an effective diffusion area of 2.54 cm². The receptor medium was filled with PBS (pH 6.5):ethanol mixture as previously used during preformulation studies. The temperature was maintained at 37 ± 0.5 °C, and the solution was continuously stirred at 180-200 rpm to ensure uniform mixing. A dialysis membrane (HiMedia Laboratories, India; MWCO 12000-14000 Da), soaked overnight for 24 h in receptor's media, was mounted between the donor and receptor compartments. The donor compartment was loaded with 1g of the optimized CUR-NG formulation. At predetermined time intervals (0.5, 1, 2, 3, and up to 24 h), 5 mL of receptor medium was withdrawn and immediately replaced with an equal volume of fresh buffer (used as media in receptor compartment) to maintain sink conditions. The collected samples were analyzed using a UV-visible spectrophotometer at the λ_{max} detected for release of curcumin [27]. *In vitro* drug release studies were conducted for the optimized nanogel and compared with a formulated conventional curcumin gel. The release data from both formulations were fitted to zero-order, first-order, Higuchi, and Korsmeyer-Peppas models to assess the release kinetics and understand the underlying drug release mechanism [36,37].

5. RESULT AND DISCUSSION

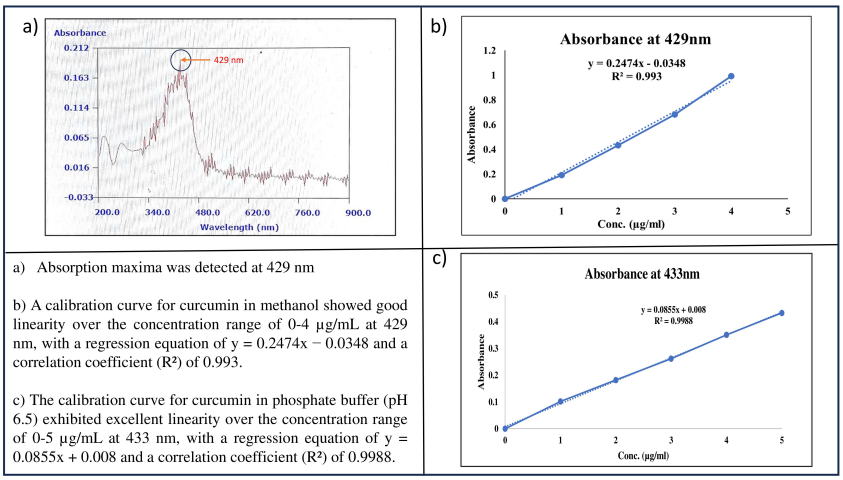
5.1 Preformulation studies

5.1.1 Assessment of melting point and organoleptic properties

Curcumin was in the form of a bright yellow, odorless, crystalline powder with a smooth texture. No visible foreign particles could be seen. The melting point of curcumin was observed at 184°C and this is in good

agreement with the reported value of 183-185°C, which confirms the crystalline nature, purity and thermal stability of curcumin.

5.1.2 UV-Vis spectrophotometer analysis



a) Absorption maxima was detected at 429 nm

b) A calibration curve for curcumin in methanol showed good linearity over the concentration range of 0-4 µg/mL at 429 nm, with a regression equation of y = 0.2474x − 0.0348 and a correlation coefficient (R^2) of 0.993.

c) The calibration curve for curcumin in phosphate buffer (pH 6.5) exhibited excellent linearity over the concentration range of 0-5 µg/mL at 433 nm, with a regression equation of y = 0.0855x + 0.008 and a correlation coefficient (R^2) of 0.9988.

Fig. 2 a) Absorption maxima validation and calibration curves of curcumin in b) methanol and c) phosphate buffer (pH 6.5)

Curcumin showed a distinct λ_{max} at 429 nm (Fig. 2a) in methanol, which is in accordance with the reported literature range of 420-430 nm, confirming its characteristic UV absorption behavior. The standard calibration curve made in methanol in 0-4 µg/mL (Fig. 2b), demonstrated perfect linearity [high correlation coefficient (R^2 = 0.993)], indicating compliance with the Beer-Lambert's law. In PBS (pH 6.5):ethanol, a slight bathochromic shift was observed with the absorption maxima shifting to 433 nm. The calibration curve (Fig. 2c) prepared in the range of 0-5 µg/mL also showed a good linearity [an excellent correlation coefficient (R^2 = 0.9988)]. These results validate the suitability of the developed UV-Vis spectrophotometric method for the precise quantitative estimation of curcumin in a methanol as well as phosphate buffer system.

5.1.3 Solubility analysis of curcumin

The solubility of curcumin was determined in various solvents to learn about solubility behavior to suit formulation. Curcumin showed very poor solubility in water (<0.001 mg/mL) and phosphate buffer (pH 6.5) (<0.005 mg/mL), which indicates poor solubility in aqueous medium. In contrast, curcumin exhibited a good degree of solubility in organic solvents by being soluble in methanol (12 mg/mL) and ethanol (9 mg/mL). A moderate solubility was seen in the mixed solvent system (7:3 ratio) of phosphate buffer pH 6.5:ethanol, in which curcumin was found to be sparingly soluble (3.1 mg/mL). These results confirm the hydrophobic character of curcumin and the need to employ advanced formulation strategies to improve curcumin solubility and bioavailability.

5.2 Preparation and selection of optimized CUR-NG

All nanogel batches were prepared according to the experimental design that was generated using the Box-Behnken design. The formulated nanogels were tested for pH and spreadability along with the selected dependent variables, i.e., particle size, zeta potential, and viscosity. Evaluation of pH was crucial to assure compatibility with the skin and to avoid skin inflammation, and spreadability evaluation was carried out to confirm ease of application and homogeneous distribution across the skin surface. Although pH and spreadability were not considered as optimization responses, the evaluation of these was essential to establish the general suitability, safety and acceptability for use. The summary of representative results of each formulation is given in Table 2.

Table 2. Physicochemical characterization of CUR-NG formulations (G1-G15)

Formulation code	Particle size (nm)	Zeta potential (mV)	Viscosity (cP)	pH	Spreadability (g·cm/s)
G1	631	-17.35	4781	4.90	2.22
G2	518	-16.70	4883	5.50	2.00
G3	620.1	-20.70	4793	5.30	1.82
G4	620	-18.90	4770	5.35	1.78
G5	630	-13.50	6568	5.07	1.74
G6	690	-18.90	4757	5.11	2.42
G7	495.5	-11.50	5420	5.47	1.38
G8	661	-14.50	5729	5.12	1.90
G9	**593**	**-18.90**	**3127**	**5.24**	**2.11**
G10	443	-16.80	4259	5.34	1.54
G11	603	-19.10	4289	4.73	1.48
G12	430	-7.90	5681	5.20	1.38
G13	649	-9.20	5501	5.33	1.60
G14	577	-9.88	5759	5.36	2.00
G15	615	-18.10	5030	5.50	1.74

5.3 ANOVA for nanogel optimization

Analysis of variance (ANOVA) was performed to determine the statistical significance of the developed models for each response. The ANOVA results (Table 3) indicated that the selected models were significant for particle size (Y_1), zeta potential (Y_2), and viscosity (Y_3), confirming the strong influence of the independent formulation variables on these key attributes of the CUR-NG.

Table 3. Model summary for optimization responses

Source of variation	F-value	p-value	R^2 value		Inference
			Predicted	Adjusted	
Y_1: Particle size					
Model: Quadratic	102.76	< 0.0001	0.9167	**0.9849**	Significant
Lack of fit	442.94	0.0549			Non-significant
Y_2: Zeta potential					
Model: Quadratic	20.92	0.0019	0.7911	**0.9741**	Significant
Lack of fit	2.61	0.7241			Not significant
Y_3: Viscosity					
Model: 2FI	39.59	< 0.0001	0.8795	**0.9674**	Significant
Lack of fit	2.09	0.3590			Not significant

5.3.1 Effect of independent variables on particle size (Y_1)

The negative coefficients of ethyl cellulose (A), Tween-80 (B), and Carbopol 940 (C) (equation 1) mean that as the concentration of these formulation variables increases, generally the particle size decreases. Among them, Tween-80 (B) showed the most influential ability, as it can reduce interfacial tension, which favors formation of smaller and uniformly dispersed particles. The positive AB and AC interaction terms indicate that a simultaneous increase in polymer and surfactant concentrations could increase system viscosity and cause restricted droplet breakup and subsequent particle growth. In contrast, negative BC interaction implies a synergistic effect between Tween-80 and Carbopol 940 and represents a further decrease in particle size. The presence of curvature of the response in the form of significant quadratic terms (B^2 and C^2) confirms the existence of a minimum particle size at certain concentrations of these variables. The quadratic polynomial equation for Y_1 is given below :

$$Y1 : 618.37 - 22.31A - 49.81B - 15.37C + 60.12AB + 18.09AC - 58.75BC - 6.37A^2 - 82.67B^2 + 26.50C^2 \ldots\ldots\ldots \text{(eqn. 1)}$$

5.3.2 Effect of independent variables on zeta potential (Y_2)

The positive values of ethyl cellulose (A) and Carbopol 940 (C) (equation 2) show an increase in concentrations of ethyl cellulose and Carbopol 940 will produce less negative zeta potential, which may lessen the effect of electrostatic repulsion between nanogel particles. In contrast, a negative coefficient of Tween-80 (B) implies that increased concentration of surfactant increases the negative surface charge and therefore improves electrostatic stabilization and dispersion stability of the nanogels. The BC interaction term suggests that a synergistic effect occurs between Tween-80 and Carbopol 940 that moderates the surface charge, resulting in reduced overall negativity and affects charge balance at the interface. The importance of the square terms (B^2 and C^2) indicates the existence of curvature in response, which would be an indication of optimization of surfactant and polymer level and is needed to obtain the desirable zeta potential values. Among the variables, Carbopol 940 had a significant influence on zeta potential (probably because it affects the viscosity of the formulation). The quadratic polynomial equation for Y_2 is given below :

$$Y2 : -19.23 + 0.8438A - 1.90B + 2.35C - 0.725AB + 1.01AC + 2.58BC - 0.692A^2 + 5.05B^2 + 2.71C^2 \ldots\ldots\ldots \text{(eqn. 2)}$$

5.3.3 Effect of independent variables on viscosity (Y_3)

The positive coefficient of ethyl cellulose (A), as depicted by equation given, indicates that increasing the concentration of ethyl cellulose leads to a corresponding effect; the viscosity is increased due to the formation of a stronger and more interconnected polymeric network. In contrast, the negative coefficient of Tween-80 (B) indicates that initially higher surfactant concentrations decrease viscosity, probably because of a reduction in polymer-polymer entanglement and an increase in molecular mobility. The positive coefficient of Carbopol 940 (C) confirms the pronounced thickening and gelling capability of Carbopol 940 in the formulation. The AB interaction term shows the effect of moderate viscosity increase, while the terms AC and BC show the strong synergy effect, leading to significant viscosity enhancement. Overall, Carbopol 940 proved to be the biggest influencing factor controlling the rheological behavior of the nanogel formulations. The quadratic polynomial equation for Y_3 is given below :

$$Y3 : 5023.13 + 204.25A - 557.38B + 574.88C + 233.25AB + 563.75AC + 703B \ldots\ldots\ldots \text{(eqn. 3)}$$

The effect of formulation variables on the critical quality attributes were further visualized by contour plots and 3D response surface methodology (RSM) plots in Fig. 3.

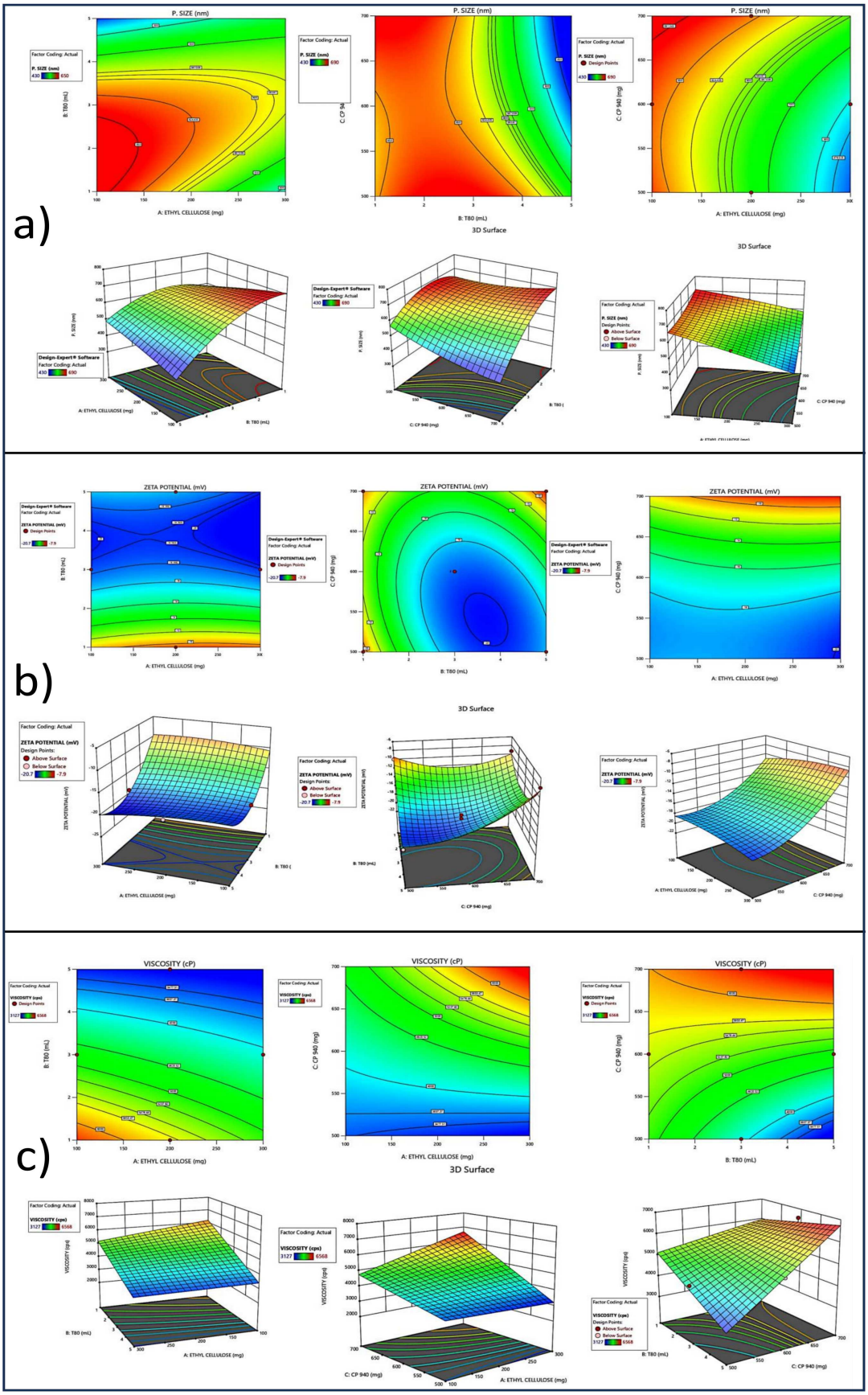


Fig. 3 2D contours and 3D RSM plots for effect of different independent variables on dependent variables a) Y_1, b) Y_2, c) Y_3

5.4 Response optimization using desirability function

The optimization strategy was set up to reduce particle size, zeta potential and viscosity, aiming to create a stable, homogeneous, and easily spreadable nanogel suitable for topical administration.

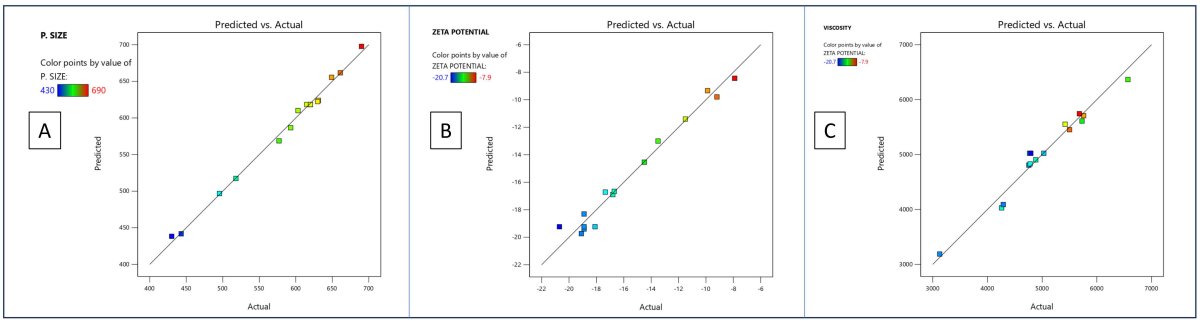


Fig. 4 Graphical comparison between actual experimental results and predicted values

The predicted versus actual plots (Fig. 4) for particle size, zeta potential, and viscosity demonstrated satisfactory agreement between the experimentally observed values and those predicted by the statistical model. In all responses, the experimental data points were distributed closely around the diagonal reference line, indicating good correlation and acceptable predictive performance of the developed model. Among the evaluated responses, particle size exhibited the strongest agreement between predicted and actual values, suggesting higher model accuracy and lower residual error for this parameter. In contrast, zeta potential and viscosity showed comparatively greater deviation from the reference line, which may be attributed to the complex influence of polymer–surfactant interactions and rheological variability within the formulation system. Nevertheless, the overall linear distribution of the data points confirmed the adequacy and reliability of the optimization model for predicting formulation responses.

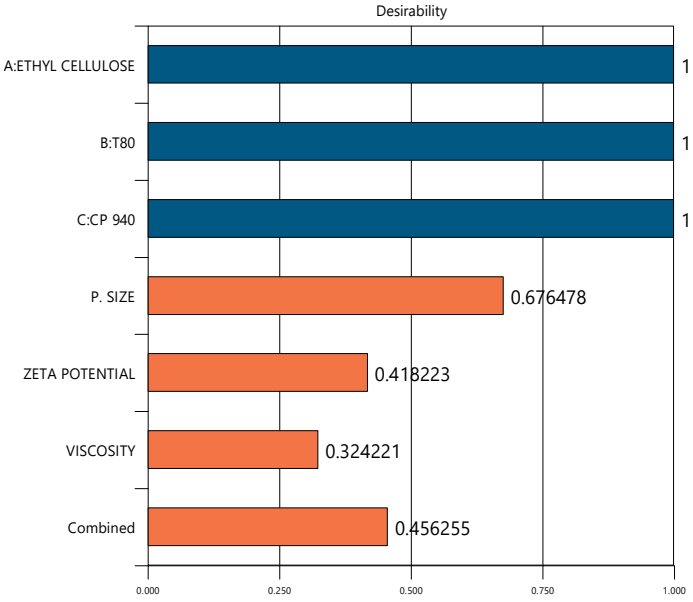


Fig. 5 Desirability plot for formulations

The desirability function plot (Fig. 5) was employed to evaluate the simultaneous optimization of formulation variables and responses. Among the evaluated responses, particle size demonstrated the highest desirability value

(0.676), suggesting comparatively better optimization and closer agreement with the targeted response criteria. In contrast, zeta potential (0.418) and viscosity (0.324) exhibited lower desirability values, indicating comparatively lesser conformity to the desired optimization goals. The overall combined desirability value of 0.456 indicated moderate optimization of the formulation and represented the best compromise solution among the evaluated experimental runs. The reduced overall desirability can be attributed to competing effects of formulation variables on colloidal stability and rheological behavior, where improvement in one response may adversely influence another response.

5.4.1 Design space analysis and selection for optimized formulation

The overlay plot (Fig.6) was generated to identify the optimum formulation region where all the selected response criteria were simultaneously satisfied. The bright yellow region represents the design space in which the particle size, zeta potential, and viscosity remained within their predetermined acceptable limits. At the fixed concentration of factor C, the overlay plot indicated that formulations containing approximately 120-220 mg of ethyl cellulose (Factor A) and 4.9-5.3 mL of Factor B satisfied the desired constraints of particle size ≤ 600 nm, zeta potential between -15 and -20.7 mV, and viscosity between 3000 and 4000 cP. Thus, the yellow design space confirms the robustness of the formulation and provides an operating region for selecting the optimized formulation with the desired physicochemical characteristics.

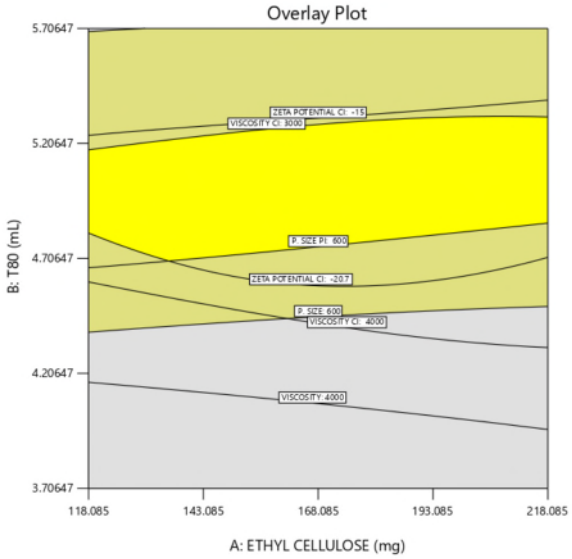


Fig. 6 Overlay plot showing the optimized design space for the formulation.

Based on point prediction analysis, optimized formulation (G9) was predicted to have particle size of 586.56 nm, zeta potential of -18.31 mV, and viscosity of 3187.88 cP. Experimental validation of the optimized batch (Table 4) provided results that were very close to the predicted values with an experimental particle size of 593nm, a zeta potential of -18.9 mV, and a viscosity of 3127 cP.

Table 4: Validation of the optimized formulation (G9): predicted versus experimental values

Response Parameter	Predicted Value	Experimental value (G9)	Deviation
Particle Size (nm)	586.56	593	+6.44 nm
Zeta Potential (mV)	-18.31	-18.90	-0.59 mV
Viscosity (cP)	3187.88	3127	-60.88 cP

This strong agreement provides the validity of the statistical soundness of the optimization process, and the effectiveness of the design of experiments (DoE) approach in achieving the desired nanogel formulation characteristics including size, PDI and zeta potential (Fig. 7).

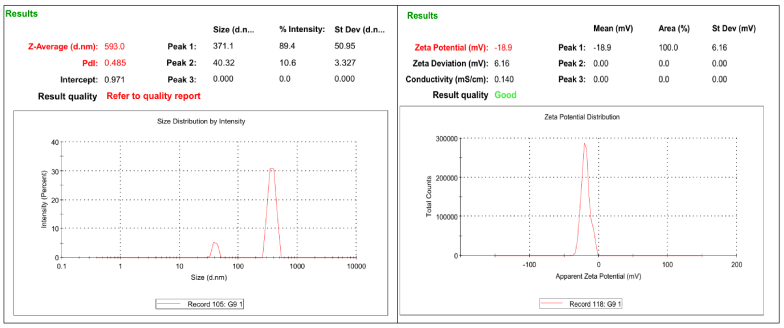


Fig. 7 Result of particle size, PDI, and zeta potential of optimized CUR-NG

5.5 Drug content of optimized nanogel

The absorbance of the diluted nanogel sample in methanol was found to be 0.139. The calibration equation (y = 0.2474x - 0.0348) was used to calculate the drug concentration, which was adjusted for dilution to calculate the total drug content. The optimized formulation exhibited 70.3% drug content, which indicates efficient drug entrapment. Minor loss of drug may be from adsorption or partial degradation during process.

5.6 FTIR compatibility analysis

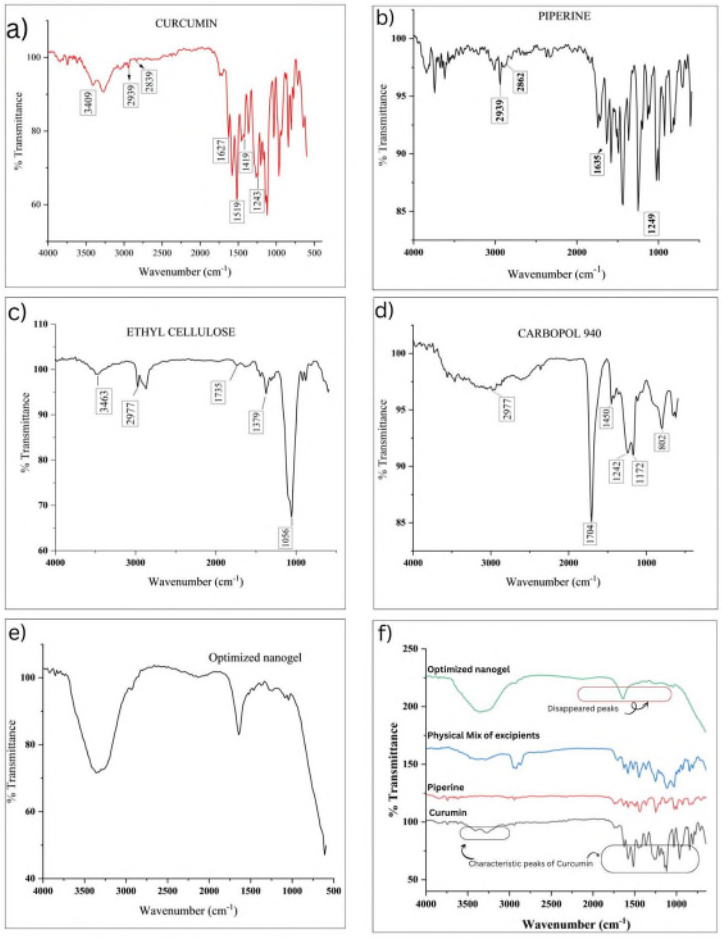


Fig. 8 FTIR analysis of a) curcumin b) piperine c) ethyl cellulose d) Carbopol 940 e) optimized nanogel (G9) f) overlay curve

The FTIR spectrum of curcumin exhibited characteristic absorption peaks at 3409 cm^{-1} (O-H stretching), 2939 cm^{-1} and 2839 cm^{-1} (aliphatic C-H stretching), 1627 cm^{-1} (conjugated C=O stretching), 1519 cm^{-1} (aromatic C=C stretching), 1419 cm^{-1} (C-OH bending), and 1243 cm^{-1} (C-O stretching), confirming its functional groups. Piperine showed prominent peaks at 2939 cm^{-1} (aromatic C-H), 2862 cm^{-1} (aliphatic C-H), 1635 cm^{-1} (C=O stretching), and 1249 cm^{-1} (C-O-C stretching). Ethyl cellulose demonstrated characteristic bands at 3463 cm^{-1} (O-H stretching), 2977 cm^{-1} (C-H stretching), 1735 cm^{-1} (ester C=O stretching), 1379 cm^{-1} (C-H bending), and 1056 cm^{-1} (C-O stretching). Carbopol 940 exhibited characteristic absorptions in the regions of 3000-2950 cm^{-1} (O-H stretching), 1750-1700 cm^{-1} (carboxylic C=O stretching), 1450-1400 cm^{-1} (C-O stretching), 1250-1200 cm^{-1} (acrylate groups), 1160 cm^{-1} (C-O-C stretching), and 850-800 cm^{-1} (=C-H bending). The respective peaks are shown in Fig. 8.

In the optimized CUR-NG, the major characteristic peaks of curcumin were diminished or appeared with reduced intensity (Fig. 8e), particularly the broadened O-H band around 3400 cm^{-1} and the preserved carbonyl peak near 1630 cm^{-1}. The absence of new peaks or disappearance of principal functional groups indicates a lack of chemical incompatibility, while the minor spectral changes suggest hydrogen bonding interactions within the polymeric matrix. These findings confirm possible encapsulation of curcumin and piperine within the nanogel system without structural degradation. Overall, overlay comparison of all components with nanogel clearly indicated chemical compatibility along with successful encapsulation.

5.7 XRD analysis

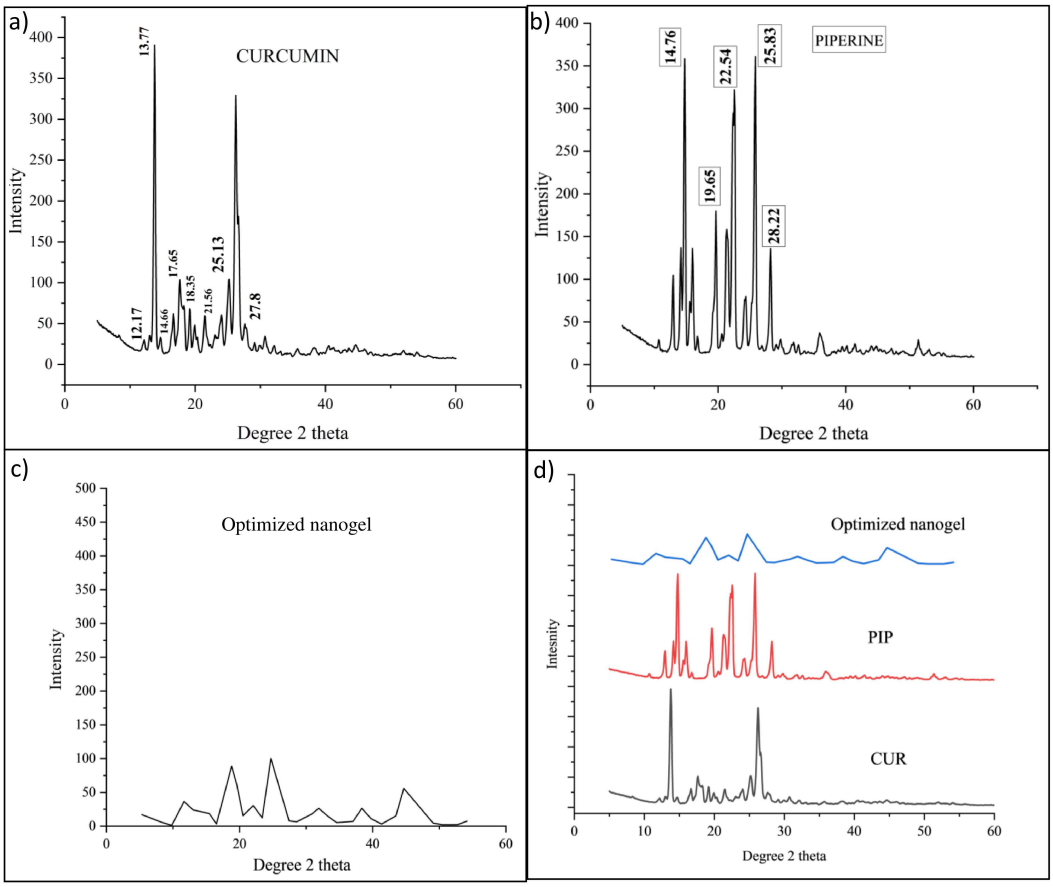


Fig. 9 XRD analysis of a) curcumin b) piperine c) optimized nanogel and d) overlay showing loss of crystallinity

Pure curcumin showed sharp and intense diffraction peaks at 12.17°, 13.77°, 14.66°, 17.65°, 18.35°, 21.56°, 25.13° and 27.80° (2θ), whereas piperine showed discrete diffraction peaks at 14.76°, 19.65°, 22.54°, 25.83° and 28.22° (2θ) (Fig. 9 a-b). In contrast, the optimized nanogel showed a wide diffused halo in the 10-60° (2θ) range with a total disappearance of the characteristic crystalline peaks (Fig. 9c). This reveals the loss of broad crystalline structure and the conversion of the drug to an amorphous phase and successful encapsulation in the polymeric nanogel matrix, which can be assessed in the overlay curve (Fig. 9d).

5.8 Differential scanning calorimetry

Pure curcumin and piperine demonstrated sharp melting endotherms (Fig. 10a-b) at 172.3 and 130.6 °C, respectively, thereby proving their crystalline nature. The deviation in the melting point of curcumin can be inherited due to the presence of minute impurities during sampling. In contrast, the optimized nanogel showed one broad endothermic peak (Fig. 10c) at 107.64 °C with the complete disappearance of the characteristic melting peaks of drug. This demonstrates crystal form of curcumin and piperine has been reduced and successful encapsulation of both in the polymeric matrix. No further thermal events up to 300 °C, illustrate good compatibility, homogeneous molecular dispersion, and thermal stability of the nanogel formulation. The overlay curve of DSC (Fig. 10d) of curcumin, piperine, and nanogel demonstrates overall encapsulation of curcumin and piperine as well as complementing XRD data of loss of crystallinity of both components.

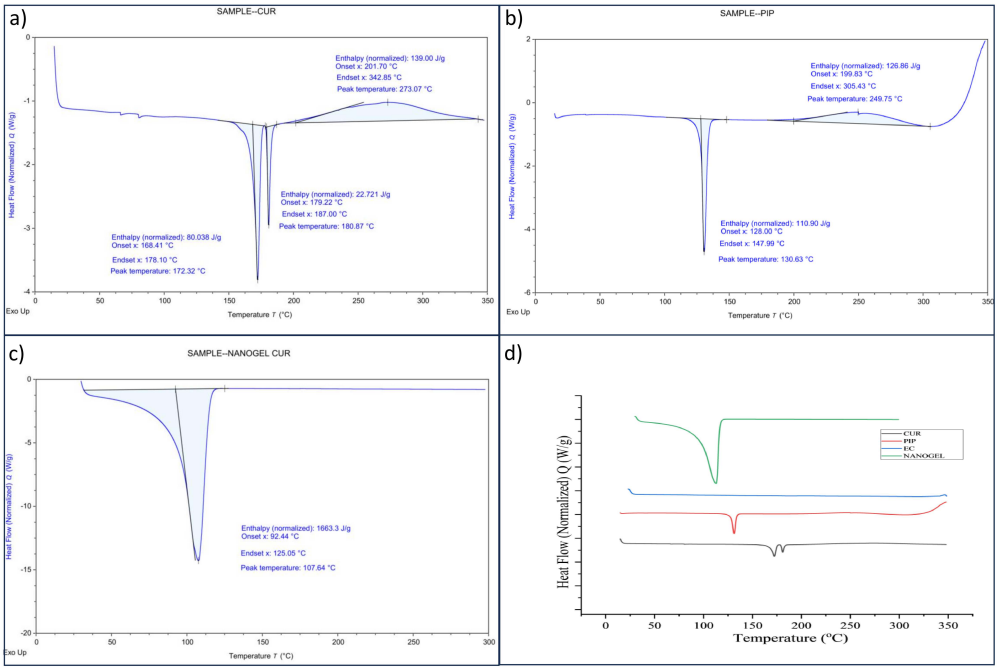


Fig. 10 XRD analysis of a) curcumin b) piperine c) optimized CUR-NG and d) overlay showing loss of crystallinity

5.9 Surface morphology of optimized CUR-NG

FESEM was carried out to determine the surface morphology and microstructural features of the optimized CUR loaded nanogel at different magnifications. At lower magnification (Fig. 11), the nanogel had a highly porous and interconnected three-dimensional structure with rough external topology. The high magnification micrograph showed that the matrix of the nanogel was composed of densely arranged and irregularly shaped nanostructures uniformly distributed in the polymeric framework. The lack of clearly visible faceted or angular crystalline domains indicates that the encapsulated drugs were molecularly dispersed or amorphized into the nanogel network

and not on the surface in crystalline form. This observation confirms the satisfactory entrapment and stabilization of curcumin and piperine in the matrix of a nano-scale matrix in the formulation and lyophilization process.

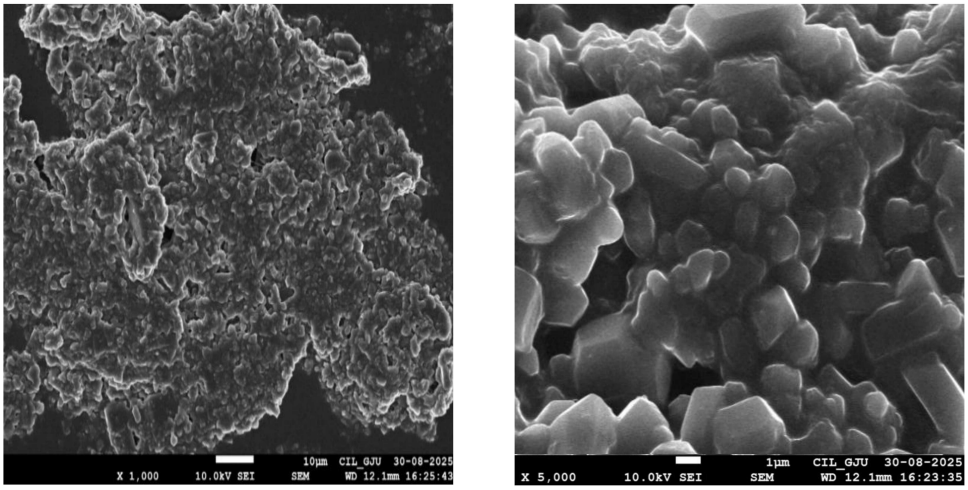


Fig. 11 FESEM analysis of lyophilized optimized CUR-NG formulation at lower magnification (x1000) and at higher magnification (x5000)

5.10 *In vitro* skin occlusivity of optimized nanogel

The *in vitro* skin occlusivity study of the optimized CUR-NG showed significant initial barrier performance. At 6 h, the control had a water loss of 1.73 g, while the optimized nanogel had a lower water loss of 0.76 g, which equates to an occlusion factor of 56.09%. This suggests adequate formation of a uniform polymeric film, which restricted transepidermal water loss and improved surface hydration. However, after 24 h, water loss for the nanogel was 3.56 g as compared to 3.97 g for the control and, therefore, a significantly decreased occlusion factor of 10.32%. The decrease in occlusivity could be explained by evaporation of the aqueous phase, the swelling-deswelling behaviour of polymers, film thinning, and the partial absorption of hydrophilic constituents into the stratum corneum.

5.11 *In vitro* antioxidant activity of optimized nanogel

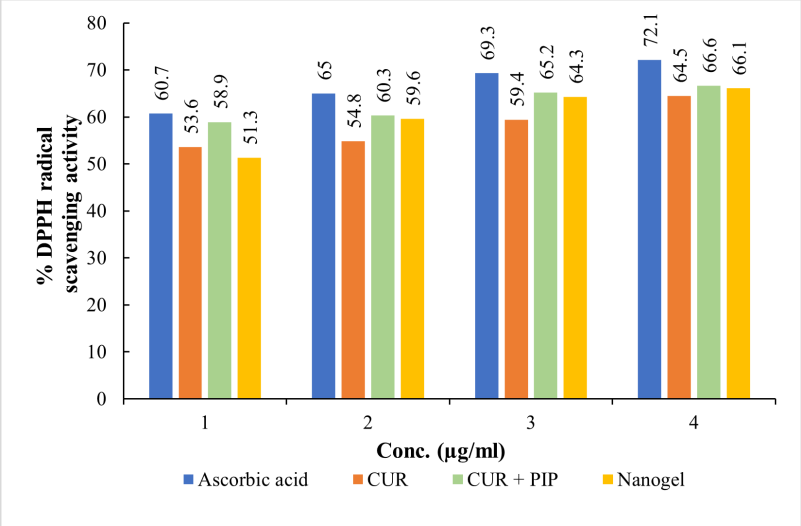


Fig. 12 Comparative representation of *in vitro* DPPH assay results

The DPPH assay (Fig. 12) showed that there is a clear concentration-dependent increase in antioxidant activity (1-4 µg/mL) for all samples. Ascorbic acid demonstrated the strongest inhibitory values of 60.7%, 65.0%, 69.3%,

and 72.1%, which proved that ascorbic acid is a potent radical scavenger. Curcumin alone had moderate activity at 53.6%, 54.8%, 59.4% and 64.5% inhibition. The combination of curcumin with piperine showed increased inhibition (58.9%, 60.3%, 65.2% and 66.6%), which is indicative of a synergetic effect of curcumin and piperine for the antioxidant effect. The optimized CUR-NG exhibited 51.3%, 59.6%, 64.3% and 66.1% inhibition at corresponding concentrations. At 4 µg/mL, nanogel (66.1%) was close to the activity of curcumin and piperine mixture (66.6%), which highlights an increase of antioxidant efficiency compared to that obtained by curcumin alone.

5.12 *In vitro* antibacterial activity

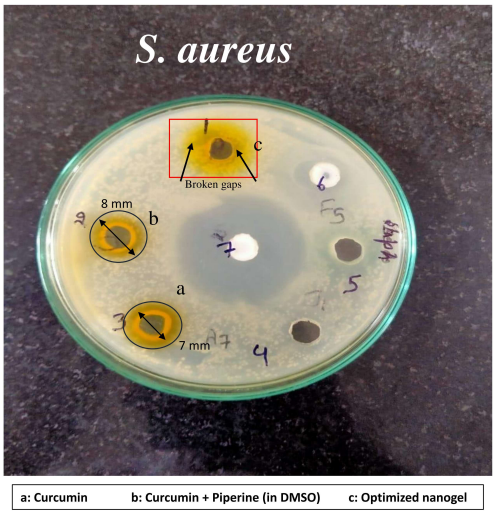


Fig. 13 Antibacterial activity of optimized CUR-NG

For *S. aureus*, curcumin and curcumin–piperine, prepared in DMSO, formulations produced zones of inhibition of 7 mm and 8 mm, respectively, as shown in Fig. 13. The developed nanogel, containing approximately 1.18 mg/ml curcumin (in DMSO), also demonstrated antibacterial activity. Although a distinct and sharply defined circular zone of inhibition was not observed, noticeable suppression and disruption of bacterial growth were evident at and around the site of application. This behavior may be attributed to the semisolid nature of the nanogel and the sustained release of curcumin from the gel matrix, which allows prolonged contact of the antibacterial agent with the bacterial cells. The observed growth inhibition confirms the antibacterial potential of the CUR-NG against *S. aureus*.

5.13 *In vitro* drug release and kinetics assessment

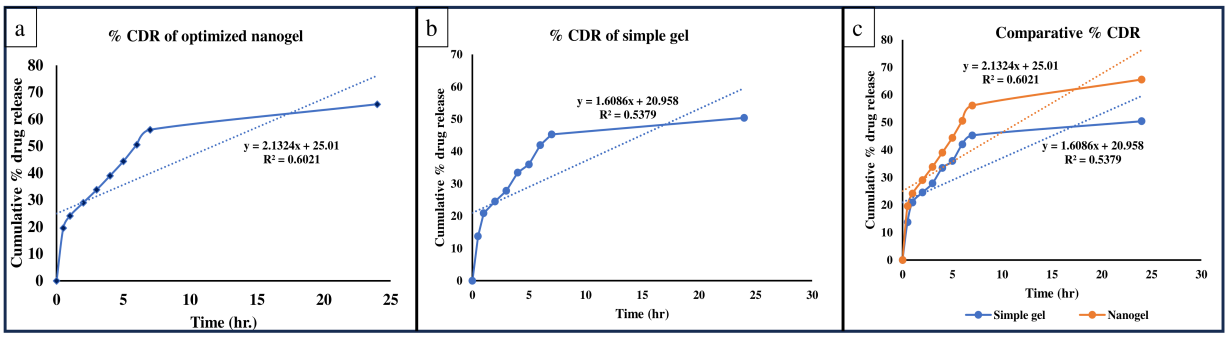


Fig. 14 a) % CDR profile of optimized CUR-NG in PBS (pH 6.5), b) % CDR profile of simple curcumin gel in PBS (pH 6.5), c) Comparative % CDR profile in PBS (pH 6.5) of both gels

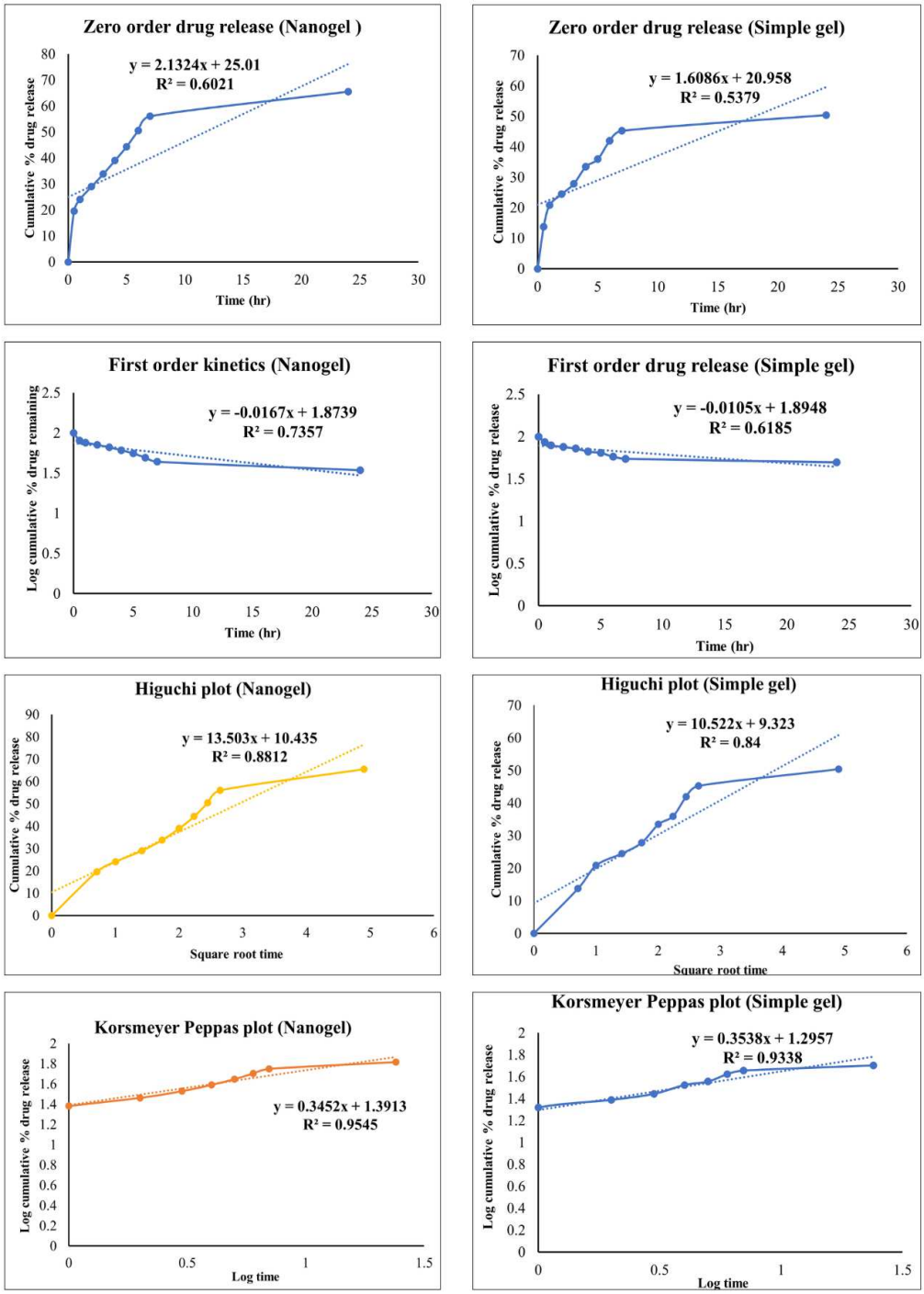


Fig. 15 Comparison of model fitting curves between optimized nanogel and simple gel

The *in vitro* release profile (Fig. 14a) of curcumin from the optimized CUR-NG showed a biphasic profile with an initial burst, further followed by sustained release. At 0.5 h, 19.59% of curcumin was released, probably because of diffusion of surface-associated or weakly entrapped drug. Release increased progressively to 24.09% (1 h), 33.80% (3 h) and 44.39% (5 h), indicating diffusion through the hydrated polymer matrix. A steady release was observed thereafter with 50.52% (6 h), 56.08% (12 h), 65.56% (24 h) confirming prolonged drug availability. The sustained release behavior can be attributed to the possible combination of the ethyl cellulose and Carbopol 940 to form a cross-linked diffusion barrier, while polyvinyl alcohol (PVA) was able to improve the matrix stability, swelling, and diffusion kinetics.

A comparative assessment of the drug release behavior between the conventional curcumin gel and the CUR-NG (Fig. 14c) was carried out to evaluate the influence of nanoscale formulation on release performance. The study revealed clear differences in the release profiles of the two systems, highlighting the impact of particle size, polymeric composition, and matrix structure on the diffusion of curcumin.

The kinetic modelling data (Fig. 15) demonstrated, that the nanogel formulation exhibited superior correlation coefficients (R^2 values) across all models compared to the simple gel, signifying a more controlled and sustained drug release behavior. Among the models evaluated (Table 5), the Korsmeyer-Peppas model ($R^2 = 0.9545$) showed the best fit for the optimized CUR-NG, indicating that the drug release mechanism primarily follows anomalous (non-Fickian) transport, governed by a synergistic interplay of diffusion and polymer relaxation. The higher R^2 values for zero-order (0.6021), first-order (0.7357), and Higuchi (0.8812) models further reinforce the enhanced uniformity and predictability of release from the nanogel matrix. Conversely, the simple gel exhibited lower R^2 values in all models, due to a comparatively fast as well as less regulated release pattern.

Table 5. Comparison between correlation coefficients (R^2) of optimized CUR-NG and simple curcumin gel

Formulation	Zero order	First order	Higuchi model	Korsmeyer-Peppas model
Nanogel	0.6021	0.7357	0.8812	0.9545
Simple gel	0.5379	0.6185	0.84	0.9338

This means, that there's an increased diffusion control and increased retention of drugs in the nanogel system. By and large, these results indicate that the nanogel formulation guarantees a longer-lasting predictable release of curcumin, which is due to its optimized polymeric network and nanoscale structure that collectively regulate the dynamics of drug diffusion and relaxation of the matrix.

6. Conclusion

This research was able to make and optimize a CUR-NG for topical treatment of psoriasis. Piperine was used in conjunction with curcumin, a BCS Class IV drug that has poor solubility, to improve its therapeutic effect. Formulation G9, which was selected via Box-Behnken Design via desirability of required parameters, had a particle size.

The optimized formulation exhibited a particle size of 593 nm, zeta potential of −18.9 mV, and viscosity of 3127 cP. Although the particle size was relatively large compared with conventional nanoemulsions, such a size range may be advantageous for topical delivery because larger droplets exhibit reduced transdermal penetration and enhanced retention within superficial skin layers, thereby favoring localized drug action [38]. Furthermore, while zeta potential values exceeding ±30 mV are generally associated with electrostatically stabilized dispersions, topical semisolid systems can achieve adequate stability through a combination of steric stabilization and increased viscosity. The optimum viscosity of the developed nanogel (3127 cP) restricts droplet mobility, minimizes collision frequency, and reduces aggregation, thereby compensating for the relatively lower zeta potential value. Similar studies have reported acceptable physical stability for topical nanoemulsions exhibiting zeta potential values around −20 mV [39]. Therefore, the obtained physicochemical characteristics are considered suitable for topical application and long-term formulation stability, which are appropriate nanoscale dimensions, stability, and topical uses. The nanogel was found to contain good drug content (70.3%) and create a semi-occlusive film at a factor of occlusion of 56.09% at 6 h, which is significant in the process of managing psoriasis

because of better hydration of the skin. Evaluation of the antioxidant attributes indicated good DPPH radical scavenging activity when compared to ascorbic acid at high concentrations, which demonstrated preserved bioactivity. There was also improved antibacterial activity of the formulation against *S. aureus*. The high sustained drug release (65.56% at 24 h) as a result of Higuchi and Korsmeyer-Peppas kinetics implies the existence of sustained local drug delivery.

Altogether, the developed nanogel demonstrated favorable physicochemical characteristics, stability, and suitability as a topical drug delivery system. The formulation exhibited promising properties that support its potential application for topical management of psoriasis; however, its therapeutic efficacy against psoriasis remains to be established through further biological evaluation. Future studies should employ psoriasis-relevant models such as *in vitro* HaCaT keratinocyte cells and *in vivo* cytokine-stimulated inflammatory models, to investigate the anti-inflammatory and anti-psoriatic potential of the formulation. Additionally, the incorporation of pH-responsive polymers may enable site-specific and controlled drug release within psoriatic lesions, potentially enhancing therapeutic performance. Successful validation of the formulation through preclinical and clinical studies could support its future translation into a commercially viable topical product and facilitate its progression from laboratory research to pharmaceutical development.

STATEMENTS AND DECLARATIONS

Competing Interests: The authors declare no competing interests.

Data Availability: Data will be made available on request.

Ethics Approval: Not applicable.

Informed Consent: None.

Funding: No funding was received to assist with the preparation of this manuscript.

References

1. Clark RA. Skin-resident T cells: the ups and downs of on site immunity. J Invest Dermatol. 2010;130:362–370. https://doi.org/10.1038/jid.2009.247
2. Kamiya K, Kishimoto M, Sugai J, Komine M, Ohtsuki M. Risk factors for the development of psoriasis. Int J Mol Sci. 2019;20:4347. https://doi.org/10.3390/ijms20184347
3. Chouhan C, Rajput RPS, Sahu R, Verma P, Sahu S. An updated review on nanoparticle based approach for nanogel drug delivery system. J Drug Deliv Ther. 2020;10:254–266. https://doi.org/10.22270/jddt.v10i5-s.4465
4. Lombardo D, Kiselev MA, Caccamo MT. Smart nanoparticles for drug delivery application: Development of versatile nanocarrier platforms in biotechnology and nanomedicine. J Nanomater. 2019;2019:3702518. https://doi.org/10.1155/2019/3702518
5. Ashraf M, El-Sawy HS, El Zaafarany GM, Abdel-Mottaleb MMA. Can essential oils/botanical agents smart-nanoformulations be the winning cards against psoriasis? Pharmaceutics. 2023;15:750. https://doi.org/10.3390/pharmaceutics15030750
6. Svenson S, Tomalia DA. Dendrimers in biomedical applications: reflections on the field. Adv Drug Deliv Rev. 2005;57:2106–2129. https://doi.org/10.1016/j.addr.2005.09.018
7. Somagoni J, Boakye CHA, Godugu C, Patel AR, Faria HAM, Zucolotto V, et al. Nanomiemgel: A novel drug delivery system for topical application: In vitro and in vivo evaluation. PLoS One. 2014;9:e115952. https://doi.org/10.1371/journal.pone.0115952
8. Zhang H, Zhai Y, Wang J, Zhai G. New progress and prospects: The application of nanogel in drug delivery. Mater Sci Eng C Mater Biol Appl. 2016;60:560–568. https://doi.org/10.1016/j.msec.2015.11.041
9. Burlec AF, Hăncianu M, Ivănescu B, Macovei I, Corciovă A. Exploring the therapeutic potential of natural compounds in psoriasis and their inclusion in nanotechnological systems. Antioxidants (Basel). 2024;13:912. https://doi.org/10.3390/antiox13080912
10. Tiatragoon W, Laffleur F, Netsomboon K. Development of curcumin-loaded lipid nanocapsules for drug delivery across mucus. J Drug Deliv Sci Technol. 2024;99:106014. https://doi.org/10.1016/j.jddst.2024.106014
11. Mohebian Z, Babazadeh M, Zarghami N. In vitro efficacy of curcumin-loaded amine-functionalized mesoporous silica nanoparticles against MCF-7 breast cancer cells. Adv Pharm Bull. 2023;13:317–327. https://doi.org/10.34172/apb.2023.035
12. Zafar A, Lahori D, Namit AF, Paxton Z, Ratna N, Thornton D, et al. Curcumin in inflammatory complications: Therapeutic applications and clinical evidence. Int J Mol Sci. 2025;26:9366. https://doi.org/10.3390/ijms26199366
13. Sharma V, Singh MK, Roy RK. Advances in phytosome technology for enhanced bioavailability of curcumin and piperine. Int J Sci Res Multidiscip Stud. 2024;10:28–35.
14. Boonyarattanasoonthorn T, Kongratanapasert T, Maiuthed A, Hamlin R, Kijtawornrat A, Khemawoot P. Bioenhancing effects of piperine and curcumin on triterpenoid pharmacokinetics and neurodegenerative metabolomes from Centella asiatica extract in beagle dogs. Sci Rep. 2022;12:20789. https://doi.org/10.1038/s41598-022-24935-7
15. Ahmad A, Akhtar J, Ahmad M, Islam A, Badruddeen, Khan MI, et al. Curcumin nanogel preparations: A promising alternative for psoriasis treatment. Curr Drug Metab. 2024;25:179–187. https://doi.org/10.2174/0113892002312605240508042634

16. Ahirwar K, Shukla R. Preformulation studies: A versatile tool in formulation design. In: Drug Formulation Design. IntechOpen; 2023. https://doi.org/10.5772/intechopen.110346
17. Kumar Majumder K, Sharma JB, Kumar M, Bhatt S, Saini V. Development and validation of UV-visible spectrophotometric method for the estimation of curcumin in bulk and pharmaceutical formulation. Pharmacophore. 2020;11:115–121.
18. Andrés A, Rosés M, Ràfols C, Bosch E, Espinosa S, Segarra V, et al. Setup and validation of shake-flask procedures for the determination of partition coefficients (log D) from low drug amounts. Eur J Pharm Sci. 2015;76:181–191. https://doi.org/10.1016/j.ejps.2015.05.008
19. N MS, S NT, R BD. Preparation and characterization of nanogel drug delivery system containing clotrimazole: An antifungal drug. Indo Am J Pharm Res. 2020.
20. Le H Van, Dulong V, Picton L, Le Cerf D. Lyophilization for formulation optimization of drug-loaded thermoresponsive polyelectrolyte complex nanogels from functionalized hyaluronic acid. Pharmaceutics. 2023;15:929. https://doi.org/10.3390/pharmaceutics15030929
21. Priyadarshini P, Karwa P, Syed A, Asha AN. Formulation and evaluation of nanoemulgels for the topical drug delivery of posaconazole. J Drug Deliv Ther. 2023;13:33–43. https://doi.org/10.22270/jddt.v13i1.5896
22. Janah H, Yulianasari DS, Azizah, Fauziyah N, Annisa R, Ahdyani R. Optimization of nano gel formulation based on Bangkal (Nauclea subdita) wood bark extract and antibacterial activity against Propionibacterium acnes. Int J Appl Pharm. 2025;17:206–213. https://doi.org/10.22159/ijap.2025v17i3.53657
23. Topuzoğlu S, Yapar EA, Abdo L, Esentürk-Güzel İ, Yurtsever AG, Gümrükçü S, et al. Optimization and characterization of khellin-loaded nanogel for the potential use in psoriasis management. Curr Pharm Biotechnol. 2025;26. https://doi.org/10.2174/0113892010375509250429052937
24. Chhajed SS, Laddha UD, Sonawane SS, Pekhale M, Thorat P, Kshirsagar SJ, et al. Formulation, development and characterization of PLGA-luliconazole nanoparticles loaded gel system for topical fungal treatment. Indian J Pharm Educ Res. 2024;58(Suppl 1):S187–S195. https://doi.org/10.5530/ijper.58.1s.18
25. Karole S, Sagar A, Chakraborty AK, Loksh KR. Formulation, development and characterization of topical organogel of mometasone furoate for the treatment of skin disease. Indian J Pharm Pharmacol. 2022;9:51–56. https://doi.org/10.18231/j.ijpp.2022.009
26. Divya, Singh I, Nagaich U. Characterisation and evaluation of prepared fluconazole nanogel for treating seborrheic dermatitis. Res J Pharm Technol. 2023;16:2880–2884. https://doi.org/10.52711/0974-360X.2023.00474
27. Tomar S, Singhal T. Formulation and evaluation of topical gel containing azithromycin and prednisolone vesicles for treating psoriasis. Int J Pharm Res Allied Sci. 2015;4:45–58.
28. Khatamsaz S, Hashemi M. Curcumin and curcumin-loaded nanogel induce apoptosis activity in K562 chronic myelogenous leukemia cells. Galen Med J. 2018;7:e921. https://doi.org/10.22086/gmj.v0i0.921
29. Kesharwani P, Jain A, Srivastava AK, Keshari MK. Systematic development and characterization of curcumin-loaded nanogel for topical application. Drug Dev Ind Pharm. 2020;46:1443–1457. https://doi.org/10.1080/03639045.2020.1793998
30. Campos LMO, Marques EM, Lera-Nonose DSSL, Gonçalves MJS, Lonardoni MVC, Nunes GC de S, et al. Enhanced nanogel formulation combining the natural photosensitizer curcumin and Pectis brevipedunculata

(Asteraceae) essential oil for synergistic daylight photodynamic therapy in leishmaniasis treatment. Pharmaceutics. 2025;17:286. https://doi.org/10.3390/pharmaceutics17030286

31. Alshehri S, Bukhari SI, Imam SS, Hussain A, Alghaith AF, Altamimi MA, et al. Formulation of piperine-loaded nanoemulsion: In vitro characterization, ex vivo evaluation, and cell viability assessment. ACS Omega. 2023;8:22406–22413. https://doi.org/10.1021/acsomega.2c08187
32. Bagheri AM, Ranjbar M, Karami-Mohajeri S, Moshafi MH, Dehghan Noudeh Y, Ohadi M, et al. Curcumin nanoemulgel: Characterization, optimization, and evaluation of photoprotective efficacy, anti-inflammatory properties, and antibacterial activity. J Clust Sci. 2024;35:2253–2272. https://doi.org/10.1007/s10876-024-02651-8
33. Rahul R, Arrivukkarasan S, Anhuradha S. In vitro antioxidant and free radical scavenging activity of Curcuma longa, Acorus calamus and Camellia sinensis. Food Nutr Sci. 2022;13:750–760. https://doi.org/10.4236/fns.2022.138054
34. Gulcin İ, Alwasel SH. DPPH Radical Scavenging Assay. Processes 2023, Vol 11, Page 2248 [Internet]. Multidisciplinary Digital Publishing Institute. 2023;11:2248. https://doi.org/10.3390/pr11082248
35. Alhelal HM, Mehta S, Kadian V, Kakkar V, Tanwar H, Rao R, et al. Solid Lipid Nanoparticles Embedded Hydrogels as a Promising Carrier for Retarding Irritation of Leflunomide. Gels [Internet]. Gels; 2023 [cited 2025 Sep 29];9. https://doi.org/10.3390/GELS9070576
36. ÇOMOĞLU T, ÇOMOĞLU T. Evaluation of Drug Release Kinetics of Temozolomide Loaded Plga Nanoparticles in Pluronic® F-127 Hydrogel. Bezmialem Science. Bezmialem Science; 2022;10:735–41. https://doi.org/10.14235/BAS.GALENOS.2022.40427
37. Roy D, Das S, Panda M, Sultana S, Mandal M, Sil I, et al. Formulation, Evaluation and Release Kinetics of Low Viscosity Metronidazole Gel with Varying Amount o f Carbopol. Indian J Sci Technol [Internet]. The Indian Society of Education and Environment; 2022;15:2690–8. https://doi.org/10.17485/IJST/V15I48.2145
38. Su R, Fan W, Yu Q, Dong X, Qi J, Zhu Q, et al. Size-dependent penetration of nanoemulsions into epidermis and hair follicles: implications for transdermal delivery and immunization. Oncotarget [Internet]. Impact Journals LLC; 2017 [cited 2026 Jun 6];8:38214. https://doi.org/10.18632/ONCOTARGET.17130
39. Rai VK, Mishra N, Yadav KS, Yadav NP. Nanoemulsion as pharmaceutical carrier for dermal and transdermal drug delivery: Formulation development, stability issues, basic considerations and applications. Journal of Controlled Release. Jun 6;270:203–25. https://doi.org/10.1016/J.JCONREL.2017.11.049